

Cerebral Amyloid Angiopathy Burden and Cerebral Microbleeds: Pathological Evidence for Distinct Phenotypes

Jonathan Graff-Radford^{a,*}, Timothy G. Lesnick^b, Michelle M. Mielke^{a,b}, Eleni Constantopoulos^c, Alejandro A. Rabinstein^a, Scott A. Przybelski^b, Prashanthi Vemuri^d, Hugo Botha^a, David T. Jones^a, Vijay K. Ramanan^a, Ronald C. Petersen^a, David S. Knopman^a, Bradley F. Boeve^a, Melissa E. Murray^f, Dennis W. Dickson^f, Clifford R. Jack^d, Kejal Kantarci^d and R. Ross Reichard^c

^aDepartment of Neurology, Mayo Clinic, Rochester, MN, USA

^bDepartment of Health Sciences Research, Mayo Clinic, Rochester, MN, USA

^cDepartment of Pathology and Laboratory Medicine, Mayo Clinic, Rochester, MN, USA

^dDepartment of Radiology, Mayo Clinic, Rochester, MN, USA

^eDepartment of Psychiatry and Psychology, Mayo Clinic, Jacksonville, FL, USA

^fDepartment of Pathology and Laboratory Medicine, Mayo Clinic, Jacksonville, FL, USA

Handling Associate Editor: M. Arfan Ikram

Accepted 12 February 2021

Pre-press 11 March 2021

Abstract.

Background: The relationship between cerebral microbleeds (CMBs) on hemosiderin-sensitive MRI sequences and cerebral amyloid angiopathy (CAA) remains unclear in population-based participants or in individuals with dementia.

Objective: To determine whether CMBs on antemortem MRI correlate with CAA.

Methods: We reviewed 54 consecutive participants with antemortem T2*GRE-MRI sequences and subsequent autopsy. CMBs were quantified on MRIs closest to death. Autopsy CAA burden was quantified in each region including leptomeningeal/cortical and capillary CAA. By a clustering approach, we examined the relationship among CAA variables and performed principal component analysis (PCA) for dimension reduction to produce two scores from these 15 interrelated predictors. Hurdle models assessed relationships between principal components and lobar CMBs.

Results: MRI-based CMBs appeared in 20/54 (37%). 10 participants had ≥ 2 lobar-only CMBs. The first two components of the PCA analysis of the CAA variables explained 74% variability. The first rotated component (RPC1) consisted of leptomeningeal and cortical CAA and the second rotated component of capillary CAA (RPC2). Both the leptomeningeal and cortical component and the capillary component correlated with lobar-only CMBs. The capillary CAA component outperformed the leptomeningeal and cortical CAA component in predicting lobar CMBs. Both capillary and the leptomeningeal/cortical components correlated with number of lobar CMBs.

Conclusion: Capillary and leptomeningeal/cortical scores correlated with lobar CMBs on MRI but lobar CMBs were more closely associated with the capillary component. The capillary component correlated with APOE ε4, highlighting lobar CMBs as one aspect of CAA phenotypic diversity. More CMBs also increase the probability of underlying CAA.

Keywords: Alzheimer's disease, capillaries, cerebral amyloid angiopathy, neuropathology

*Correspondence to: Jonathan Graff-Radford, MD, Mayo Clinic, 200 First Street SW, Rochester, MN 55905, USA. Tel.: +1 507 284 2511; Fax: +1 507 538 6012; E-mail: graff-radford.jonathan@mayo.edu.

+1 507 284 2511; Fax: +1 507 538 6012; E-mail: graff-radford.jonathan@mayo.edu.

INTRODUCTION

In population-based studies, cerebral microbleeds (CMBs) detected on hemosiderin-sensitive MRI sequences increase with age with a prevalence of ~40% for those over the age of 80 years [1–3]. Several studies have shown the clinical relevance of CMBs, which are associated with risk of future hemorrhage [4, 5], cognitive decline [6], and increased mortality [7]. CMBs are also important safety variables in Alzheimer's disease clinical trials. In the context of Alzheimer's disease clinical trials, CMBs form one component of amyloid imaging-related abnormalities (ARIA-H) [8].

Prior studies have shown that cerebral amyloid angiopathy (CAA) pathology [9] contributes to development of lobar CMBs detected on MRI [10]. In the Boston Criteria for CAA, the presence of two or more lobar-only hemorrhages, including lobar CMBs, has high specificity for the disease [11, 12]. These criteria were validated in a small number of community-based individuals with two or more lobar CMBs, but only 25% had at least moderate CAA at autopsy [11, 13, 14]. Therefore, a better understanding of the relationship between CMBs and CAA pathology is necessary in populations without macrohemorrhages including those who may be enrolled in AD clinical trials to minimize potential for morbidity. CAA pathological criteria assess CAA burden in both leptomeningeal and cortical vessels and determine the presence or absence of capillary CAA [15]. The objectives of this study were to determine the association between post-mortem CAA burden and antemortem MRI-detected CMBs and to determine which aspects of CAA pathology were associated with CMBs.

MATERIALS AND METHODS

Participants

All individuals in this study were enrolled in either the Mayo Clinic Study of Aging (MCSA) or the Mayo Alzheimer's Disease Research Center (ADRC). The MCSA is a population-based study among Olmsted County, Minnesota, residents evaluating risk factors for cognitive impairment [16]. The Mayo Alzheimer's Disease Research Center (ADRC) is a longitudinal research study of individuals recruited from clinical practice. Age and sex were self-reported at the in-person clinical examination. Clinical syndrome duration was from symptom onset to death. All

individuals without a medical contraindication are invited to participate in imaging studies. In October 2011, T2^{*} GRE was introduced into the research protocol. Participants included in this study underwent a brain MRI between October 2011 and June 2016, which included a T2^{*}-GRE sequence, and subsequently came to autopsy regardless of clinical or pathological diagnosis.

APOE allele status (carrier versus non-carrier) was determined through standard genotyping methods on blood samples [17].

Both studies were approved by the Mayo Clinic and Olmsted Medical Center Institutional Review Boards. Written informed consent was obtained from all participants and/or their surrogates.

MRI acquisition

All images were obtained using 3-tesla MRI scanners (GE). The complete details of the acquisitions were previously published [2]. In brief, a T2^{*} GRE was performed with the following parameters: repetition time/echo time = 200/20 ms; flip angle = 12°; in-plane matrix = 256 × 224; phase field of view = 1.00; and slice thickness = 3.3 mm. On the MRI, CMBs were defined according to consensus criteria [18] as homogeneous hypointense lesions in the gray or white matter, which are distinct from iron or calcium deposits and vessel flow voids on T2^{*} GRE images. The CMB grading has previously been described in detail [2, 19, 20]. All CMBs were identified by trained image analysts and confirmed by a vascular neurologist (JGR) experienced in interpreting the T2^{*} GRE images. When it was not possible to distinguish a CMB definitively from a flow void, the CMB was recorded as a "possible CMB." Possible CMBs were excluded from analysis. The intra-rater reliability based on blinded reading on two separate occasions was excellent (κ statistic 0.86). The interrater agreement between a neuroradiologist and neurologist on definite versus not-definite CMB was 87%, corresponding to good agreement (κ 0.68). The location of each CMB was recorded in the coordinate system of the image on which it was made by the rater. A structural T1 magnetization-prepared rapid gradient echo image of the participant was registered and resampled into the GRE image. An in-house, modified automated anatomic-labeling atlas delineated lobar regions and deep/infratentorial gray and white matter regions [21]. CMBs were classified as lobar-only (with or without cerebellar CMBs) or deep/infratentorial CMBs (with or without cerebellar

CMBs). Mixed CMBs were those with at least 1 lobar and 1 deep CMB. For participants who underwent multiple MRI scans, the scan closest to autopsy was used.

Neuropathology

Neuropathologic sampling followed recommendations of the Consortium to Establish a Registry for Alzheimer's Disease (CERAD) [22]. Regions sampled included anterior cingulate and posterior cingulate gyri, anterior hippocampus, posterior hippocampus (level of the lateral geniculate nucleus), middle-frontal gyrus, inferior parietal lobule, superior and middle temporal gyri, primary visual/visual association cortices, nucleus basalis, amygdala, striatum, midbrain, and cerebellum. CERAD plaque score was assessed in each region. An antibody to A β (6F/3D, 1:100, human A β 8-17 Dako monoclonal mouse anti-human beta-amyloid) was used to stain each section on formalin-fixed, paraffin-embedded tissue.

CAA scoring

CAA burden was graded according to the Love Consensus Criteria [15] by a board-certified neuropathologist. Regions graded for CAA burden included

frontal, parietal, temporal, occipital, and hippocampal regions. Missing data by region were as follows: Frontal $n=3$, temporal $n=1$, parietal $n=2$, visual $n=1$, hippocampal $n=4$. According to the grading scale, CAA burden was rated in the leptomeningeal and parenchymal areas for each region on a 0–3 scale (0 = absent CAA; 1 = scant CAA; 2 = involvement of ≥ 2 arterioles, some with circumferential A β ; and 3 = widespread arteriolar A β deposition, many of which were circumferential (Fig. 1). Capillary CAA was rated as present or absent (Fig. 2).

Statistical analysis

Demographic and clinical characteristics of the participants were summarized using means and SDs for continuous variables and counts and percentages for categorical variables. Distributions of the continuous variables were examined for approximate symmetry and normality using plots. Using a heat map with default hierarchical clustering, we examined the relationship between cortical, leptomeningeal, and capillary CAA across participants. Because our data set included a large set (15) of highly related predictors, we then ran several types of principal component analysis (PCA) to reduce the dimensionality and

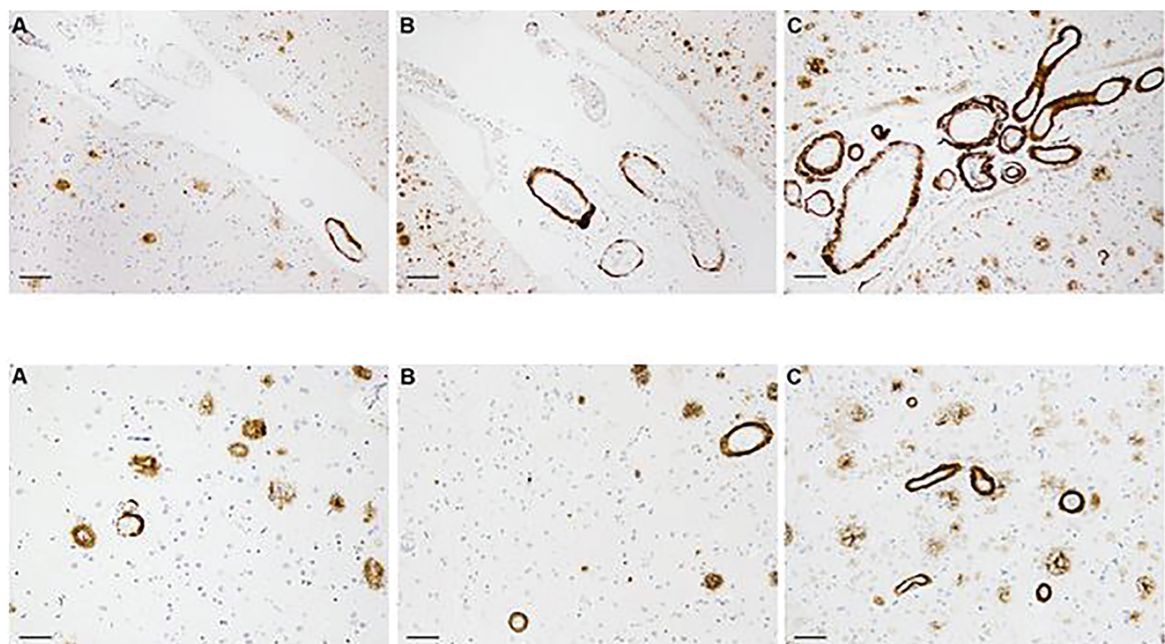


Fig. 1. Representative sections immunostained with A β show CAA scores of increasing severity, graded on a scale of 0–3, in leptomeningeal (top row) and parenchymal (bottom row) vessels. CAA score 0 is not depicted. Panel A show CAA score 1 with sparse positively-stained vessels. Moderate severity in Panel B represent CAA score 2, with A β deposition in several vessels and some with circumferential staining. Panel C show CAA score 3 with widespread, circumferential vascular positivity. Extracellular A β plaque formation within the cortex is also demonstrated. Scale bars represent 100 μ m.

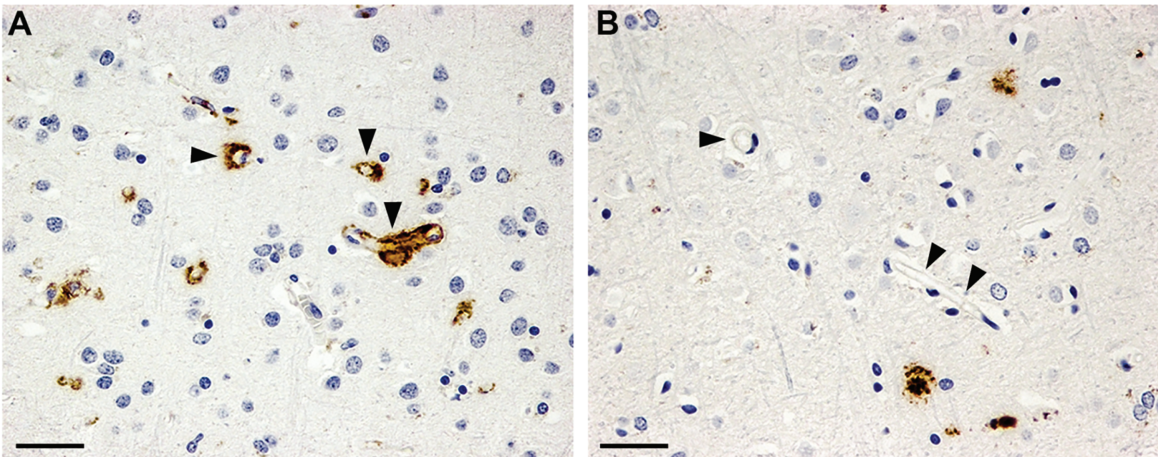


Fig. 2. A β immunostaining demonstrating presence or absence of capillary CAA. A) Arrowheads indicate A β deposition in capillaries. B) Arrowheads indicate uninvolved capillaries. Minimal parenchymal A β plaque formation is present. Scale bars represent 50 μ m.

de-correlate many CAA measures. Variables were standardized for PCA, and all 15 variables were included in the analyses. Since we had both binary and continuous variables, we settled on a PCA of mixed data using the R function PCAmix [23] analysis as our final method, though all PC analyses produced similar results. PCAmix [23] is a data-reduction method similar to ordinary PCA but distinguishes ordinal/continuous variables from categorical variables. If all variables are continuous, it reduces to ordinary PCA; if all variables are categorical, it reduces to multiple-correspondence analysis. We restricted to the first two components (eigenvalues 9.54 and 1.50, other eigenvalues were < 1.00), and a Varimax rotation was applied to the first two PCAmix components to improve interpretation. We report the significant loadings after rotation.

Using the rotated PCAmix results, we produced two scores rotated component (RPC)1 (cortical/leptomeningeal) and RPC2 (capillary) by standardizing each variable and then calculating weighted sums multiplying each standardized variable by the corresponding loading (each RPC is thus a weighted sum).

We additionally ran hurdle models [24, 25] to examine the association of CAA with CMBs (total or lobar only). Hurdle models analyze data with an excess of zeros, as is frequently the case for count data such as CMBs.

The hurdle models consisted of two components: 1) a logistic regression model to predict the presence of one or more CMBs versus 0 CMBs, which constitutes the hurdle; and 2) a truncated Poisson model for predicting number of lobar CMBs among those with

CMBs. A truncated negative binomial model was also considered as an alternative to the truncated Poisson, but examination of the results and rootograms comparing observed and expected frequencies showed little difference between the two. We report coefficients, standard errors, and p -values for the hurdle models. For the logistic regressions, the coefficients estimate log odds ratios of at least one CMB versus not, and for ease of interpretation, we also report odds ratios (OR) and 95% confidence intervals (CI). For the truncated Poisson, the coefficients estimate change in the log counts, and the exponentiated coefficients estimate incidence rate ratios (IRR). Thus, for a one-unit change in the predictor variable, the difference in the logs of expected counts is expected to change by the coefficient, given that other predictors in the model are held constant. We adjusted for time between the CMB measurement and death (time to death) in all of the models.

RESULTS

The demographics of the study participants and primary pathological diagnosis are summarized in Table 1. Three participants had a history of intracranial hemorrhage. Two were traumatic (subdural), and one was a spontaneous thalamic hemorrhage with intraventricular extension, which was clinically diagnosed as a hypertensive hemorrhage.

Cerebral microbleeds were present in 20/54 participants (mixed deep and lobar = 1, deep only = 2, lobar only = 17). Ten participants had 2 or more lobar-only CMBs. Over half had at least one *APOE* ε4 allele.

Table 1
Demographics of study participants ($n=54$)

Male, no. (%)	41 (76%)
Age, y	72.7 (11.2)
<i>APOE ε4</i> carrier, no. (%)	28 (53%)
<i>APOE ε2</i> carrier, no. (%)	4 (8%)
Education, y	15.4 (2.8)
MMSE at MRI	19.3 (7.5)
Death Age, y	74.8 (11.3)
Time from scan to death, y	2.1 (1.0)
Clinical diagnosis at MRI	
Cognitively unimpaired, no. (%)	12 (22%)
Mild cognitive impairment, no. (%)	3 (6%)
Dementia no. (%)	39 (72%)
Any CMB present, no. (%)	20 (37%)
None	34 (63%)
1 CMB	9 (17%)
2 CMB	6 (11%)
3 + CMB	5 (9%)
Lobar CMB present, no. (%)	18 (33%)
Deep CMB present, no. (%)	3 (6%)
Primary pathological diagnosis	
Alzheimer's disease, no. (%)	30 (56%)
Argyrophilic grain disease, no. (%)	1 (2%)
FTLD (TDP-43), no. (%)	7 (13%)
FTLD tau, no. (%)	2 (4%)
Lewy body disease, no. (%)	11 (20%)
Primary age-related tauopathy, no. (%)	2 (4%)
Prion disease, no. (%)	1 (2%)
Clinical syndrome duration, y	10.3 (4.3)
Alzheimer disease research center, no. (%)	38 (70%)
Mayo clinic study of aging, no. (%)	16 (30%)

Characteristics table with the mean (SD) listed for the continuous variables and count (%) for the categorical variables. FTLD, frontotemporal lobar degeneration.

Table 2 summarizes the regional CAA burden of leptomeningeal and cortical CAA.

The heat map with default hierarchical clustering (Fig. 3) demonstrated that cortical and leptomeningeal CAA burden travel together and distinctly from capillary CAA burden.

PCA results

The cumulative percent of variability in the CAA variables explained by the first two principal components was approximately 74% (Fig. 4). After applying a varimax rotation to make interpreting the results easier, the first component consisted of cortical/leptomeningeal CAA and the second component of capillary CAA (see Table 3).

Relationship with lobar CMBs

Scatterplots of RPC1 (cortical/leptomeningeal) and RPC2 (capillary) versus lobar-only CMBs looked similar, showing an increasing trend in lobar CMBs

Table 2
Distribution of CAA severity by location

CAA severity	Frontal		Temporal		Parietal		Occipital		Hippocampus	
	Cort	Lepio	Cap	Cort	Lepio	Cap	Cort	Lepio	Cap	Cort
None, no. (%)	26 (51%)	20 (39%)	44 (86%)	31 (58%)	23 (43%)	48 (91%)	33 (63%)	26 (50%)	43 (83%)	27 (51%)
Mild, no. (%)	12 (24%)	12 (24%)	—	13 (25%)	17 (32%)	—	10 (19%)	14 (27%)	—	14 (26%)
Moderate, no. (%)	5 (10%)	6 (12%)	—	5 (9%)	5 (9%)	—	4 (8%)	7 (13%)	—	2 (4%)
Severe, no. (%)	8 (16%)	13 (25%)	—	4 (8%)	8 (15%)	—	5 (10%)	5 (10%)	—	10 (19%)
										11 (21%)
										7 (14%)
										3 (6%)
										7 (14%)

Capillary CAA is a dichotomous variable (present/absent). % absent presented above. Cort, cortical; Lepio, leptomeningeal; Cap, capillary.

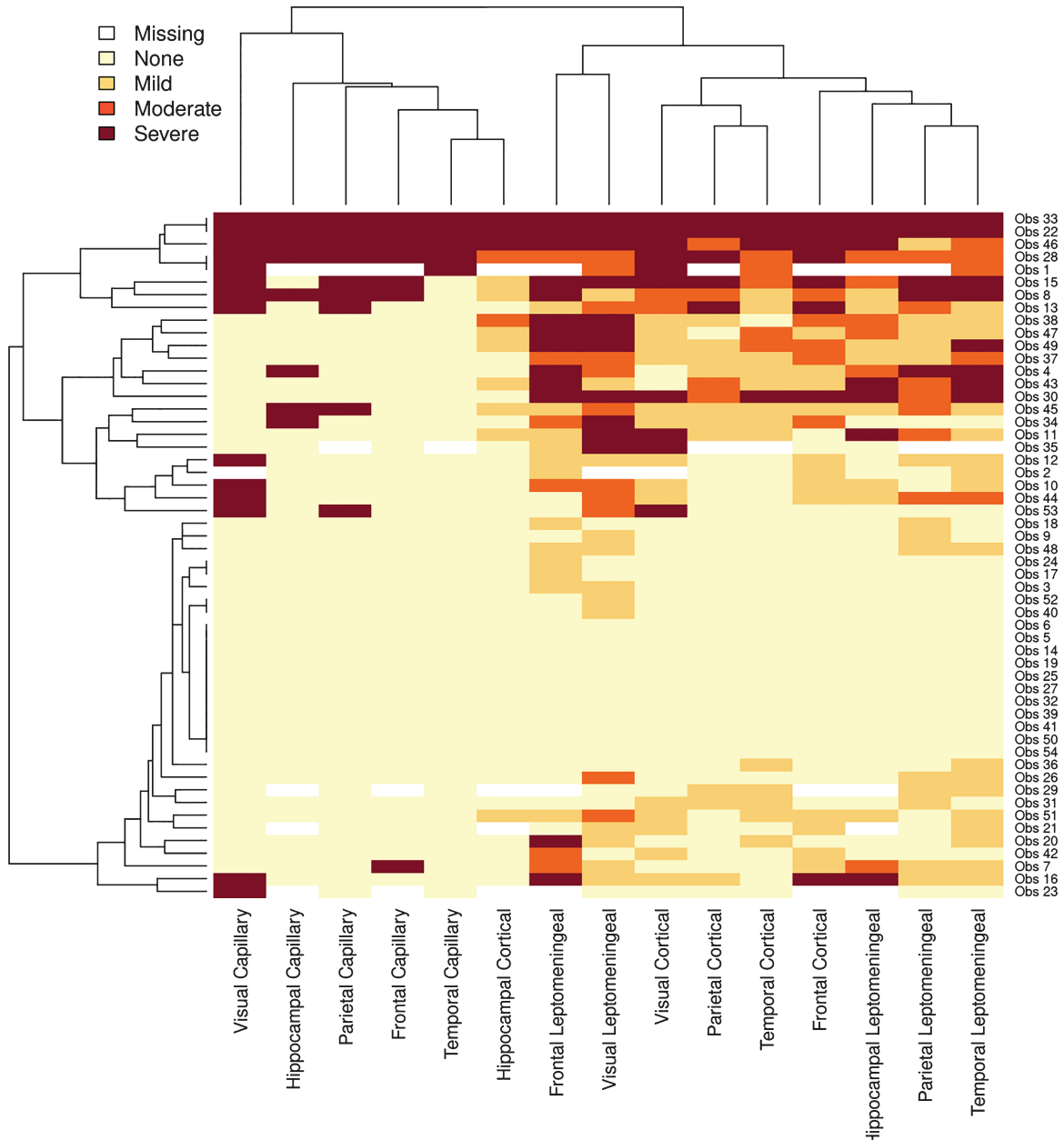


Fig. 3. Heat map of CAA severity with a dendrogram at the top and left side based on hierarchical clustering that uses complete linkage method to group items on how similar they are to each other.

with higher values of RPC1 and RPC2. Two participants with >10 CMBs had the highest values for cortical/leptomeningeal and capillary components. However, most participants with zero CMBs had low capillary component scores but were spread out more with cortical/leptomeningeal scores. In this particular sample, the capillary component separated lower from higher counts of lobar better than the cortical/leptomeningeal component. Adjusting for age

made no difference in the models, and age was never significant as a predictor. The rotated components correlated with each other, with a Pearson correlation coefficient of about 0.75.

Using lobar CMBs as the outcome and cortical/leptomeningeal and capillary components as predictors, adjusting for time to death, CAA scores were unassociated with the presence or absence of a CMB. However, both cortical/leptomeningeal and

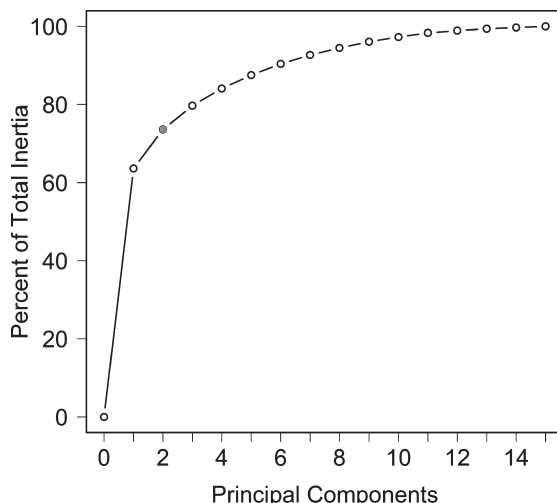


Fig. 4. Principal component analysis explaining variability.

Table 3

Loadings for first two components of PCAmix analysis after Varimax rotation

RPC2 (capillary)	
Visual cortex capillary CAA	0.48
Hippocampus capillary CAA	0.49
Parietal lobe capillary CAA	0.75
Frontal lobe capillary CAA	0.62
Temporal lobe capillary CAA	0.70
RPC1 (leptomeningeal/cortical)	
Hippocampus cortical CAA	0.26
Frontal lobe leptomeningeal CAA	0.74
Visual cortex leptomeningeal CAA	0.64
Visual cortex cortical CAA	0.33
Parietal lobe cortical CAA	0.46
Temporal lobe cortical CAA	0.53
Frontal lobe cortical CAA	0.58
Hippocampus leptomeningeal CAA	0.73
Parietal leptomeningeal CAA	0.54
Temporal leptomeningeal CAA	0.75

capillary components were associated with the number of lobar CMBs among those with at least one CMB (Table 4). Therefore, CAA was not associated with the presence of a CMB, but amongst those with CMBs, higher CAA scores correlated with more CMBs. When both cortical/leptomeningeal and capillary components were entered in the same model, the capillary component was significant but cortical/leptomeningeal was not. This likely reflects the multicollinearity between the two components and that the capillary component performed slightly better than RPC1. Hurdle models using total CMBs as the outcome showed very similar results. Adjusting the models for age did not significantly change

the results. Two individuals had a high number of lobar CMBs (> 10) and potentially skewed the results. However, removing those individuals from the analyses did not qualitatively change the results.

DISCUSSION

This study had several key findings. First, our clustering and PCA analyses suggest that capillary versus cortical/leptomeningeal involvement reflect non-identical aspects of CAA with differential relationships to CMBs. Second, we found no evidence that CMB development during a lifetime was itself associated with overall postmortem CAA burden. However, among individuals with ≥ 1 CMB, higher overall CAA burden correlated with higher numbers of lobar CMBs, consistent with the concept that a greater burden of CMBs increases the likelihood of underlying CAA.

Thal proposed the existence of two forms of sporadic CAA, which differ by the presence of capillary CAA involvement. Capillary CAA involvement was more associated with the presence of Alzheimer's disease pathology [26]. Our results support Thal's findings, since our PCA analysis found the variability in CAA could largely be explained by two components: cortical/leptomeningeal CAA and the presence of capillary CAA. Reciprocally, the pathologic phenotypes support the emerging data from clinical studies of heterogeneity in how CAA manifests clinically [27].

Recently, several studies have highlighted different clinical phenotypes of CAA by *APOE* allele status. *APOE* ε2 has been associated with cortical superficial siderosis, convexity subarachnoid hemorrhage, and higher future lobar intracerebral hemorrhage risk, while *APOE* ε4 has been associated with lobar cerebral microbleeds [27–30]. Our finding that capillary CAA was more strongly (as compared with cortical/leptomeningeal CAA) associated with lobar cerebral microbleeds indirectly reinforces prior data linking *APOE* ε4 specifically with capillary CAA [26, 31]. If our cohort had participants with cortical superficial siderosis, which is characterized by leptomeningeal hemosiderin deposition, we might have seen a stronger relationship to leptomeningeal CAA and a diverging relationship between cortical and leptomeningeal CAA. A recent imaging-pathological study demonstrated that the pathological correlate of cortical superficial siderosis was predominantly leptomeningeal CAA [32]. Our study adds to prior

Table 4
Hurdle models predicting lobar-only CMBs using rotated principal components

Outcome	Variable	Coefficient (s.e.)	OR (95% CI) or IRR (95% CI)	<i>p</i>
Capillary (RCP1) only				
CMB (Y/N)	Intercept	-1.29 (0.86)	0.28 (0.05–1.49)	0.134
	Time to death	0.16 (0.35)	1.174 (0.59–2.33)	0.647
	PCAmix capillary	0.22 (0.13)	1.250 (0.98–1.60)	0.076
CMB (No.)	Intercept	0.04 (0.42)	1.04 (0.46–2.37)	0.923
	Time to death	0.27 (0.13)	1.310 (1.01–1.70)	0.045
	PCAmix capillary	0.22 (0.04)	1.249 (1.15–1.34)	<0.001
Lep/cortical (RCP2) only				
CMB (Y/N)	Intercept	-1.12 (0.83)	0.33 (0.06–1.65)	0.174
	Time to death	0.09 (0.34)	1.10 (0.57–2.12)	0.787
	PCAmix lep/cortical	0.09 (0.07)	1.09 (0.96–1.25)	0.186
CMB (No.)	Intercept	0.392 (0.413)	1.48 (0.66–3.33)	0.342
	Time to death	0.144 (0.133)	1.16 (0.89–1.50)	0.276
	PCAmix lep/cortical	0.134 (0.030)	1.14 (1.08–1.21)	<0.001
Both capillary (RCP1) and lep/cortical (RCP2)				
CMB (Y/N)	Intercept	-1.28 (0.86)	0.28 (0.05–1.49)	0.134
	Time to death	0.16 (0.35)	1.17 (0.59–2.33)	0.647
	PCAmix capillary	0.22 (0.18)	1.25 (0.87–1.80)	0.224
CMB (No.)	PCAmix lep/cortical	0.001 (0.10)	1.00 (0.82–1.22)	0.995
	Intercept	-0.07 (0.44)	0.94 (0.39–2.22)	0.879
	Time to death	0.318 (0.15)	1.37 (1.03–1.83)	0.031
CMB (No.)	PCAmix capillary	0.32 (0.13)	1.38 (1.06–1.77)	0.016
	PCAmix lep/cortical	-0.07 (0.09)	0.93 (0.79–1.11)	0.421

CMB, cerebral microbleed; OR, odds ratio; IRR, incidence rate ratio; No., number; lep/cortical, leptomeningeal/cortical.

radiologic-pathologic correlation studies and confirms the utility of the Boston Criteria for detecting CAA pathology *in vivo* in individuals without CAA clinical features, such as lobar intracerebral hemorrhage or amyloid spells. Further, our data suggest that confidence in a CAA diagnosis increases with greater numbers of lobar-only CMBs. However, the presence of a single CMB, even if in the lobar region, does not necessarily implicate CAA as the underlying substrate. This non-specificity of a single lobar CMB supports prior studies and has implications for AD clinical trials [14]. Thal demonstrated that capillary CAA is associated with carrying an *APOE ε4* allele. Since carrying an *APOE ε4* allele is associated with lobar CMBs, this fits with our current findings that lobar CMBs correlate with capillary CAA pathology.

This study has several limitations. We used a convenience cohort of individuals recruited from the Alzheimer's Disease Research Center to participate in research and a population-based study; therefore, our findings are not generalizable to all with CAA pathology. The fairly small available sample size might additionally limit stability/reproducibility of the loadings from the PCA, and power to detect associations with CMB. These limitations add to the importance of follow-up studies. Because the majority of participants were on the AD spectrum, lobar

CMBs were more common than deep CMBs. In addition, participants underwent T2* MRI imaging, which is less sensitive for CMB detection than SWI. Including individuals with predominantly vascular cognitive impairment (higher burden of deep CMBs) or with other clinical and imaging manifestations of CAA, such as superficial siderosis, clinical lobar hemorrhage, and/or convexity subarachnoid hemorrhage, may have changed our results as well as the principal components identified.

These data advance our understanding of CAA endo-phenotypes and may help explain the distinct clinical and neuroimaging presentations of CAA observed in clinical practice.

ACKNOWLEDGMENTS

Research reported in this publication was supported by the National Institute on Aging of the National Institutes of Health (NIH) under Award Number K76AG057015 and the NIH (AG006786, AG011378, NS097495, AG16574), and the GHR Foundation. The funders had no role in the conception or preparation of this manuscript.

Authors' disclosures available online (<https://www.j-alz.com/manuscript-disclosures/20-1536r2>).

REFERENCES

- [1] Vernooij MW, van der Lugt A, Ikram MA, Wielopolski PA, Niessen WJ, Hofman A, Krestin GP, Breteler MMB (2008) Prevalence and risk factors of cerebral microbleeds: The Rotterdam Scan Study. *Neurology* **70**, 1208-1214.
- [2] Graff-Radford J, Botha H, Rabinstein AA, Gunter JL, Przybelski SA, Lesnick T, Huston J, 3rd, Flemming KD, Preboske GM, Senjem ML, Brown RD, Jr., Mielke MM, Roberts RO, Lowe VI, Knopman DS, Petersen RC, Kremers W, Vemuri P, Jack CR, Jr., Kantarci K (2019) Cerebral microbleeds: Prevalence and relationship to amyloid burden. *Neurology* **92**, e253-e262.
- [3] Romero JR, Preis SR, Beiser A, DeCarli C, Viswanathan A, Martinez-Ramirez S, Kase CS, Wolf PA, Seshadri S (2014) Risk factors, stroke prevention treatments, and prevalence of cerebral microbleeds in the Framingham Heart Study. *Stroke* **45**, 1492-1494.
- [4] Wilson D, Ambler G, Shakeshaft C, Brown MM, Charidimou A, Al-Shahi Salman R, Lip GHY, Cohen H, Banerjee G, Houlden H, White MJ, Yousry TA, Harkness K, Flossmann E, Smyth N, Shaw LJ, Warburton E, Muir KW, Jager HR, Werring DJ (2018) Cerebral microbleeds and intracranial haemorrhage risk in patients anticoagulated for atrial fibrillation after acute ischaemic stroke or transient ischaemic attack (CROMIS-2): A multicentre observational cohort study. *Lancet Neurol* **17**, 539-547.
- [5] van Etten ES, Auriel E, Haley KE, Ayres AM, Vashkevich A, Schwab KM, Rosand J, Viswanathan A, Greenberg SM, Gurol ME (2014) Incidence of symptomatic hemorrhage in patients with lobar microbleeds. *Stroke* **45**, 2280-2285.
- [6] Akoudad S, Wolters FJ, Viswanathan A, de Brujin RF, van der Lugt A, Hofman A, Koudstaal PJ, Ikram MA, Vernooij MW (2016) Association of cerebral microbleeds with cognitive decline and dementia. *JAMA Neurol* **73**, 934-943.
- [7] Benedictus MR, Prins ND, Goos JD, Scheltens P, Barkhof F, van der Flier WM (2015) Microbleeds, mortality, and stroke in Alzheimer disease: The MISTRAL Study. *JAMA Neurol* **72**, 539-545.
- [8] Sperling RA, Jack CR, Jr., Black SE, Frosch MP, Greenberg SM, Hyman BT, Scheltens P, Carrillo MC, Thies W, Bednar MM, Black RS, Brashear HR, Grundman M, Siemers ER, Feldman HH, Schindler RJ (2011) Amyloid-related imaging abnormalities in amyloid-modifying therapeutic trials: Recommendations from the Alzheimer's Association Research Roundtable Workgroup. *Alzheimers Dement* **7**, 367-385.
- [9] Schrag M, McAuley G, Pomakian J, Jiffry A, Tung S, Mueller C, Vinters HV, Haacke EM, Holshouser B, Kido D, Kirsch WM (2010) Correlation of hypointensities in susceptibility-weighted images to tissue histology in dementia patients with cerebral amyloid angiopathy: A postmortem MRI study. *Acta Neuropathol* **119**, 291-302.
- [10] Fazekas F, Kleinert R, Roob G, Kleinert G, Kapeller P, Schmidt R, Hartung HP (1999) Histopathologic analysis of foci of signal loss on gradient-echo T2*-weighted MR images in patients with spontaneous intracerebral hemorrhage: Evidence of microangiopathy-related microbleeds. *AJNR Am J Neuroradiol* **20**, 637-642.
- [11] Knudsen KA, Rosand J, Karluk D, Greenberg SM (2001) Clinical diagnosis of cerebral amyloid angiopathy: Validation of the Boston criteria. *Neurology* **56**, 537-539.
- [12] Greenberg SM, Charidimou A (2018) Diagnosis of cerebral amyloid angiopathy. *Stroke* **49**, 491-497.
- [13] van Rooden S, van der Grond J, van den Boom R, Haan J, Linn J, Greenberg SM, van Buchem MA (2009) Descriptive analysis of the Boston criteria applied to a Dutch-type cerebral amyloid angiopathy population. *Stroke* **40**, 3022-3027.
- [14] Martinez-Ramirez S, Romero J-R, Shoamanesh A, McKee AC, Van Etten E, Pontes-Neto O, Macklin EA, Ayres A, Auriel E, Himali JJ, Beiser AS, DeCarli C, Stein TD, Alvarez VE, Frosch MP, Rosand J, Greenberg SM, Gurol ME, Seshadri S, Viswanathan A (2015) Diagnostic value of lobar microbleeds in individuals without intracerebral hemorrhage. *Alzheimers Dement* **11**, 1480-1488.
- [15] Love S, Chalmers K, Ince P, Esiri M, Attems J, Jellinger K, Yamada M, McCarron M, Minett T, Matthews F, Greenberg S, Mann D, Kehoe PG (2014) Development, appraisal, validation and implementation of a consensus protocol for the assessment of cerebral amyloid angiopathy in post-mortem brain tissue. *Am J Neurodegener Dis* **3**, 19-32.
- [16] Roberts RO, Geda YE, Knopman DS, Cha RH, Pankratz VS, Boeve BF, Ivnik RJ, Tangalos EG, Petersen RC, Rocca WA (2008) The Mayo Clinic Study of Aging: Design and sampling, participation, baseline measures and sample characteristics. *Neuroepidemiology* **30**, 58-69.
- [17] Hixon JE, Vernier DT (1990) Restriction isotyping of human apolipoprotein E by gene amplification and cleavage with HhaI. *J Lipid Res* **31**, 545-548.
- [18] Greenberg SM, Vernooij MW, Cordonnier C, Viswanathan A, Al-Shahi Salman R, Warach S, Launer LJ, Van Buchem MA, Breteler MM (2009) Cerebral microbleeds: A guide to detection and interpretation. *Lancet Neurol* **8**, 165-174.
- [19] Graff-Radford J, Aakre JA, Knopman DS, Schwarz CG, Flemming KD, Rabinstein AA, Gunter JL, Ward CP, Zuk SM, Spychalla AJ, Preboske GM, Petersen RC, Kantarci K, Huston J, 3rd, Jack CR, Jr., Mielke MM, Vemuri P (2020) Prevalence and heterogeneity of cerebrovascular disease imaging lesions. *Mayo Clin Proc* **95**, 1195-1205.
- [20] Graff-Radford J, Lesnick T, Rabinstein AA, Gunter J, Aakre J, Przybelski SA, Spychalla AJ, Huston J, 3rd, Brown RD, Jr., Mielke MM, Lowe VI, Knopman DS, Petersen RC, Jack CR, Jr., Vemuri P, Kremers W, Kantarci K (2020) Cerebral microbleed incidence, relationship to amyloid burden: The Mayo Clinic Study of Aging. *Neurology* **94**, e190-e199.
- [21] Vemuri P, Gunter JL, Senjem ML, Whitwell JL, Kantarci K, Knopman DS, Boeve BF, Petersen RC, Jack CR, Jr. (2008) Alzheimer's disease diagnosis in individual subjects using structural MR images: Validation studies. *Neuroimage* **39**, 1186-1197.
- [22] Mirra SS, Heyman A, McKeel D, Sumi SM, Crain BJ, Brownlee LM, Vogel FS, Hughes JP, van Belle G, Berg L (1991) The Consortium to Establish a Registry for Alzheimer's Disease (CERAD). Part II. Standardization of the neuropathologic assessment of Alzheimer's disease. *Neurology* **41**, 479-486.
- [23] Chavent M, Kuentz-Simonet V, Labenne A, Saracco J (2014) Multivariate analysis of mixed data: The R Package PCAMixdata. *arXiv preprint arXiv:1411.4911*.
- [24] Mullahy J (1986) Specification and testing of some modified count data models. *J Econom* **33**, 341-365.
- [25] Zeileis A, Kleiber C, Jackman S (2008) Regression models for count data in R. *J Stat Softw* **27**, doi: 10.18637/jss.v027.i08.
- [26] Thal DR, Ghebremedhin E, Rüb U, Yamaguchi H, Del Tredici K, Braak H (2002) Two types of sporadic cerebral amyloid angiopathy. *J Neuropathol Exp Neurol* **61**, 282-293.
- [27] Charidimou A, Boulous G, Gurol ME, Ayata C, Bacska BJ, Frosch MP, Viswanathan A, Greenberg SM (2017) Emerging concepts in sporadic cerebral amyloid angiopathy. *Brain* **140**, 1829-1850.

- [28] Charidimou A, Martinez-Ramirez S, Shoamanesh A, Oliveira-Filho J, Frosch M, Vashkevich A, Ayres A, Rosand J, Gurol ME, Greenberg SM, Viswanathan A (2015) Cerebral amyloid angiopathy with and without hemorrhage: Evidence for different disease phenotypes. *Neurology* **84**, 1206-1212.
- [29] Pichler M, Vemuri P, Rabinstein AA, Aakre J, Flemming KD, Brown RD, Jr., Kumar N, Kantarci K, Kremers W, Mielke MM, Knopman DS, Jack CR, Jr., Petersen RC, Lowe V, Graff-Radford J (2017) Prevalence and natural history of superficial siderosis: A population-based study. *Stroke* **48**, 3210-3214.
- [30] Yost M, Fiebelkorn CA, Rabinstein AA, Klaas J, Aakre JA, Brown RD, Jr., Mielke MM, Knopman DS, Lowe V, Petersen RC, Jack CR, Jr., Vemuri P, Graff-Radford J (2019) Incidence of convexal subarachnoid hemorrhage in the elderly: The Mayo Clinic Study of Aging. *J Stroke Cerebrovasc Dis* **28**, 104451.
- [31] Richard E, Carrano A, Hoozemans JJ, van Horssen J, van Haastert ES, Eurelings LS, de Vries HE, Thal DR, Eikelenboom P, van Gool WA, Rozemuller AJ (2010) Characteristics of dyshoric capillary cerebral amyloid angiopathy. *J Neuropathol Exp Neurol* **69**, 1158-1167.
- [32] Charidimou A, Perosa V, Frosch MP, Scherlek AA, Greenberg SM, van Veluw SJ (2020) Neuropathological correlates of cortical superficial siderosis in cerebral amyloid angiopathy. *Brain* **143**, 3343-3351.